Journal Pre-proof

Active chitosan/gum Arabic-based emulsion films reinforced with thyme oil encapsulating blood orange anthocyanins: Improving multi-functionality

Runan Zhao, Jin Chen, Songfeng Yu, Ruihao Niu, Zhehao Yang, Han Wang, Huan Cheng, Xingqian Ye, Donghong Liu, Wenjun Wang

Please cite this article as: Zhao, R., Chen, J., Yu, S., Niu, R., Yang, Z., Wang, H., Cheng, H., Ye, X., Liu, D., Wang, W., Active chitosan/gum Arabic-based emulsion films reinforced with thyme oil encapsulating blood orange anthocyanins: Improving multi-functionality, *Food Hydrocolloids* (2022), doi: https://doi.org/10.1016/j.foodhyd.2022.108094.
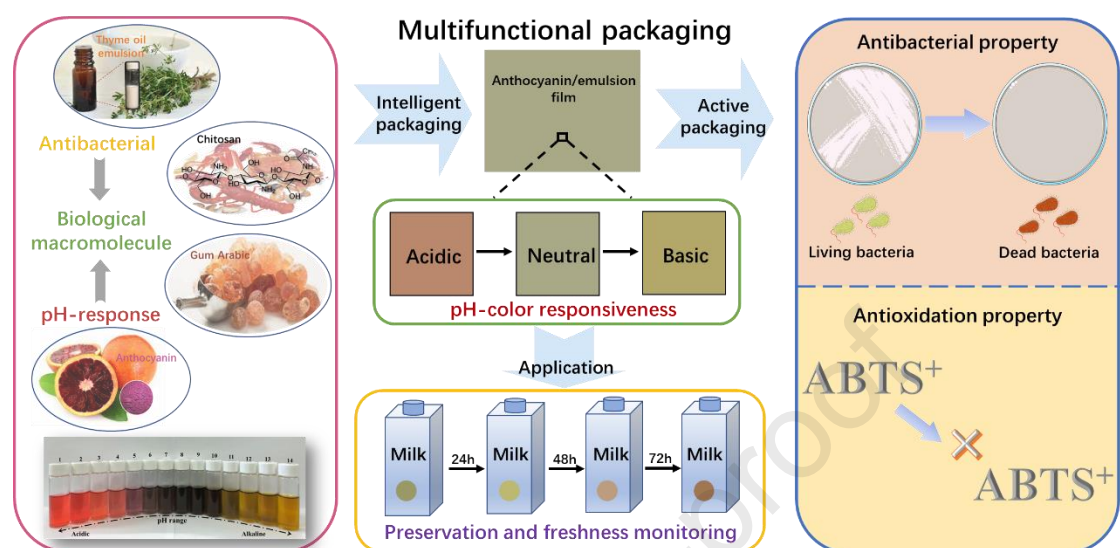
This is a PDF file of an article that has undergone enhancements after acceptance, such as the addition of a cover page and metadata, and formatting for readability, but it is not yet the definitive version of record. This version will undergo additional copyediting, typesetting and review before it is published in its final form, but we are providing this version to give early visibility of the article. Please note that, during the production process, errors may be discovered which could affect the content, and all legal disclaimers that apply to the journal pertain.

CRediT authorship contribution statement

Runan Zhao: Conceptualization, Methodology, Investigation, Formal analysis, Software, Data curation, Writing-original draft. **Jin Chen**: Methodology and analysis. **Songfeng Yu**: Formal analysis. **Ruihao Niu**: Software. **Zhehao Yang**: Investigation. **Han Wang**: Investigation. **Huan Cheng**: Supervision. **Xingqian Ye**: Supervision. **Donghong Liu**: Writing-review & editing, Funding acquisition. **Wenjun Wang**: Supervision, Writing-review & editing.

Graphical abstract

1 **Active chitosan/gum Arabic-based emulsion films reinforced with**

2 **thyme oil encapsulating blood orange anthocyanins: Improving multi-**

3 **functionality**

4 Runan Zhao [a], Jin Chen [a], Songfeng Yu [a], Ruihao Niu [a], Zhehao Yang [a], Han Wang [a],

5 Huan Cheng [a, b, c], Xingqian Ye [a, b, c], Donghong Liu [a, b, c], Wenjun Wang [a, b, c]*

6 [a] *College of Biosystems Engineering and Food Science, Zhejiang University,*

7 *Hangzhou 310058, China*

8 [b] *Fuli Institute of Food Science, Zhejiang University, Hangzhou, 310058, China*

9 [c] *Ningbo Research Institute, Zhejiang University, Ningbo 315100, Zhejiang, China*

10

11 * Corresponding author. Address: No 866 Yuhangtang Road, Xihu District, Hangzhou

12 310058, China, E-mail: wangwj@zju.edu.cn

13

Abstract

Novel multifunctional food packaging was developed by incorporating blood orange anthocyanins (BOA) and thyme oil (TO) emulsion into a chitosan-gum Arabic film matrix. The basic properties, pH/volatile acid sensitivity, and functional characteristics of the multifunctional films were investigated. BOA solution illustrated significant color variations (from pink to violet to yellow) under different pH environments. The incorporation of anthocyanin and emulsion enhanced the UV-vis blocking, which made the film block almost all UV light. Meanwhile, the multifunctional film had stronger mechanical strength and thermal stability, whose elongation at break reached 76.1%, and the maximum degradation temperature raised to 305°C. The incorporation of TO emulsion significantly enhanced the films' water resistance and made the water vapor barrier properties of the films reduce to 6.34×10^{-11} g/Pa•h•m. In addition, the multifunctional films exhibited noticeable changes of color in acid/alkaline environments within a short time interval, which could be easy to distinguish by naked eyes. The addition of emulsion made the multifunctional films slow-release of thyme oil, which significantly improved the antioxidant and dynamic antibacterial capacity of the films. Finally, the multifunctional films effectively extended the shelf-life of milk at 25°C and visually monitored freshness through the color changes in real-time. This knowledge provides a new perspective and idea to develop multifunctional food packaging materials with preservation and monitoring functions.

35   **Keywords:** multifunctional packaging, anthocyanins, thyme oil emulsion, pH-

36   sensitivity, colorimetric indicator, food preservation

37

1. Introduction

In response to the growing concerns of consumers about food safety, sustainability, and environmental impact, new advanced biodegradable, active and intelligent food packaging materials have attracted extensive attention from researchers in the food industry (Alizadeh Sani, Tavassoli, Salim, Azizi-lalabadi, & McClements, 2022). Among them, intelligent packaging is designed to monitor changes in environmental conditions and food ingredients during storage in real time, and then provide naked eyes with readable signals, such as color changes (Mohammadian, Alizadeh-Sani, & Jafari, 2020; Pirsa, Sani, & Mirtalebi, 2022). Furthermore, consumers can quickly distinguish the freshness of internal food without opening the package, improving food quality and reducing food waste (Sani, Tavassoli, Hamishehkar, & McClements, 2021; Zhang, et al., 2021). Active packaging can be designed to maximize its functional performance by adding antibacterial agents and antioxidants, which can prevent food from spoilage during storage (Sani et al., 2021; Azman, Khairul, & Sarbon, 2022). Thyme oil is a volatile aromatic substance extracted from thyme, which has excellent antioxidant and broad-spectrum antibacterial activity (Zhang et al., 2021).

Anthocyanins are a family of plant-derived, non-toxic, biodegradable, water-soluble pigments with excellent antioxidant and antibacterial activities (Fernández-Marín, Fernandes, Sánchez, & Labidi, 2022). Importantly, anthocyanins have a sensitive color response to a wide range of acid-base changes due to the alterations in their conjugated structure (Pirsa, Sani, & Mirtalebi, 2022; Wu et al., 2019). Blood

59 orange (*Citrus sinensis* L. Osbeck) is the only commercial citrus fruit containing

60 anthocyanins (Carmona, Alquezar, Marques, & Pena, 2017). In addition to providing a

61 unique color among citrus fruits, blood orange anthocyanins (BOA) are also related to

62 human health because of their antioxidant activity (Habibi, et al., 2022). At present,

63 there are many studies about developing food packaging films based on citrus

64 processing products and wastes (Yun & Liu, 2022). However, the potential

65 practicability of BOA in the development of intelligent packaging has not yet been

66 reported. Consequently, BOA, as the source of "blood" in blood orange, can be used as

67 an antioxidant and colorimetric sensor in intelligent packaging materials, which can be

68 applied to monitor the food quality by changing color in response to changes in food

69 pH or other characteristics (Becerril, Nerín, & Silva, 2021; Huang, et al., 2022; Neves,

70 Andrade, Videira, de Freitas, & Cruz, 2022; Roy & Rhim, 2021a).

71   Many essential oils are "generally recognized as safe" (GRAS) food additives and

72 can be used as natural antibacterial agents in the food industry (Zhao et al., 2020;

73 Mukurumbira, Shellie, Keast, Palombo, & Jadhav, 2022). Because of its high

74 hydrophobicity and volatility, researchers developed an emulsion encapsulation system

75 based on ultrasonic treatment to improve its stability and antibacterial activity (Guo et

76 al., 2020; Yang, He, Ismail, Hu, & Guo, 2022). The emulsifier is adsorbed on the surface

77 of oil and water, which form a protective layer to protect the essential oil from external

78 influences (Zhao et al., 2020). At the same time, the essential oil can be slowly released

79 from the emulsion, which also gives the film a slow-release effect on the essential oil

80　when the emulsion was incorporated into the film (Zhang, Jiang, Rhim, Cao, & Jiang,

81　2022). Hereby, the essential oil emulsion can be used as an antibacterial agent to

82　improve the physical and functional properties of films (Zhang et al., 2021;

83　Mukurumbira, et al., 2022).

84　　　From an environmental point of view, these packaging films made from natural

85　biological macromolecules (such as proteins and polysaccharides) have green,

86　environmental-friendly and biodegradable advantages over petroleum-based films

87　(Atta, et al., 2022; Chen, et al., 2022). Chitosan (CS) is a polycationic polysaccharide

88　derived from chitin after deacetylation and has been widely used in food packaging

89　systems because of its nontoxicity, great biocompatibility, biodegradability, and film-

90　forming properties (Zhao, Zhang, Chen, Song, & Li, 2022). Gum Arabic (GA), a natural

91　polyanionic heteropolysaccharide extracted from the branches or trunks of Acacia trees,

92　can interact with polycationic polymers such as chitosan (Xu et al., 2019). Therefore,

93　chitosan/gum Arabic nanocomposite films are expected to show better functional

94　properties.

95　　　To sum up, the development of novel intelligent and active multifunctional food

96　packaging films has excellent potential, whose ultimate goal is to improve food safety,

97　quality, and sustainability. Hence, the objective of this research was to fabricate a novel

98　biodegradable multifunctional food packaging, using chitosan and gum Arabic to

99　assemble the film matrix, BOA as pH indicators, and thyme oil emulsion to provide an

100　antibacterial and slow-release effect to improve the shelf-life of food (**Fig. 1**). The

101   influence of anthocyanin and emulsion on films' physical properties and structure were

102   investigated. Meanwhile, the pH and volatile acids sensitivity, as well as essential oil

103   release characteristics, were determined. Furthermore, the antioxidant and antibacterial

104   activity of multifunctional films were also measured. Finally, the practical application

105   effect of multifunctional films on milk preservation and freshness monitoring was

106   investigated.

107   **2. Materials & methods**

108   **2.1. Materials**

109   Thyme essential oil (TO, W306540) was obtained from Sigma-Aldrich (St. Louis,

110   MO, USA). Cinnamaldehyde (CA, purity $\geq$ 98%) was purchased from Aladdin Reagent

111   Co. (Shanghai, China). Chitosan (CS, MW 280 kDa, degree of deacetylation = 85%)

112   was purchased from Zhejiang Golden-Shell Pharmaceutical Co. (Zhejiang, China).

113   Gum Arabic (GA, MW 250 kDa) was provided by the G-GLONE Biotechnology Co.

114   (Beijing, China). Polyvinyl alcohol (PVA, 1799) and glycerol were purchased by

115   RHAWN Co. (Shanghai, China). Nutritional agar (NA), and nutritional broth (NB)

116   were obtained from Gaoke Haibo biotechnology Co., Ltd (Qingdao, China). Three

117   different brands of pasteurized milk were purchased from Wal-Mart Supermarket

118   (Hangzhou, China). Chemicals other than those used in this study were of analytical

119   grade.

120   **2.2. Extraction of anthocyanins from blood orange**

121   Anthocyanins were isolated from blood oranges using the method with some

122 modifications (Kim, Roy, & Rhim, 2022). After the blood oranges flesh was

123 homogenized, the sample was extracted with anhydrous ethanol in the dark for 24 h at

124 25°C. Afterward, the sample was filtered and centrifuged at 6000×g for 15 min. The

125 supernatant was collected, filtered, and concentrated by removing the ethanol using a

126 rotary evaporator (50°C). The sample was adsorbed overnight with D101 macroporous

127 adsorption resin in a dark place. After that, the sample was eluted with 60% ethanol at

128 pH 3, and the eluent was rotary-evaporated at 50°C. Then, the eluent was extracted with

129 ethyl acetate and concentrated by a rotary evaporator (50°C) again. Finally, the extract

130 solution was freeze-dried and the anthocyanin extract powders were obtained. The total

131 anthocyanin content in the obtained powders was (176.35 ± 1.2) mg/g, determined by

132 the pH difference method (Chen, Yan, Huang, Zhou, & Hu, 2021).

133 **2.3. Fabrication of thyme oil emulsion**

134   A two-step emulsification method was used to fabricate thyme oil emulsion (Yang

135 et al., 2022; Zhao et al., 2020). TO (4 wt% in the emulsion) and cinnamaldehyde (CA,

136 2.5 wt% in the oil phase) were mixed evenly as the oil phase. The aqueous phase was

137 composed of CS (0.2 wt%) and PVA (2 wt%) at pH 6.5. Firstly, the oil and water mixture

138 were homogenized by a high-speed homogenizer (FJ200-S; Lichen Instrument

139 Technology Co. Ltd, Hunan, China) at 12,000 rpm for 3 min in an ice bath to get a

140 coarse emulsion. Secondly, the coarse emulsion was sonicated by a 20 kHz ultrasonic

141 processor (Scientz-II D; Ningbo Scientz, Zhejiang, China) at 450 W in the ice bath for

142 10 min (ultrasound 5 s, pause 5 s) and adjusted pH to 4 to formulate the final emulsion.

2.4. Fabrication of multifunctional films

Initially, the CS/GA solution was prepared by mixing chitosan (2 wt%) and gum Arabic (2 wt%) solution, evenly stirring for 2 h. Subsequently, anthocyanins (1 mg/mL and 3 mg/mL) were added into CS/GA solution with continual stirring. After that, the emulsion (keeping the concentration of thyme oil in film at 20 mg/g) was added into the polysaccharide solution, and 0.5 wt% glycerol was served as a plasticizer. The emulsion in the control group was replaced by distilled water. Ultimately, the 25 mL film-forming solutions were cast on a Petri dish (15 cm × 15 cm) and dried for 48 h in a dark air vacuum oven (35℃). The final films were stored with 50% RH at 25℃ in a dark place before analysis. For the sake of convenience, the final films were labeled as CS/GA, A-CS/GA, E-CS/GA, 1A-E-CS/GA, and 3A-E-CS/GA. "CS/GA" was the chitosan/gum Arabic film, "A-CS/GA" was the chitosan/gum Arabic film with 3 mg/mL anthocyanin content, "E-CS/GA" was the TO emulsion-chitosan/gum Arabic film, "1A-E-CS/GA" and "3A-E-CS/GA" were the TO emulsion-chitosan/gum Arabic films with 1 mg/mL and 3 mg/mL anthocyanin content.

2.5. Colorimetry and optical properties of multifunctional films

2.5.1. Color coordinates

The color change of the films under different pHs was determined with the colorimeter (CR-10, Konica Minolta, Tokyo, Japan). Briefly, the films were immersed in different buffer solutions (pH 3.0-13.0) for 10 min. The appearance of films was captured, and the parameters of color were recorded. The total color difference (ΔE)

164 was calculated as follows:

165 $$\Delta E = \sqrt{(L_1 - L_2)^2 + (a_1 - a_2)^2 + (b_1 - b_2)^2} \qquad (1)$$

166 where L_1, a_1, and b_1 represented the color parameters of each film. L_2 (94.61), a_2 (-1.36),

167 and b_2 (-0.17) were the standard white screen's color coordinates.

2.5.2. UV-vis barrier performance and transparency

169 The UV-vis barrier performance and transparency of the films were evaluated

170 through an ultraviolet spectrophotometer (UV-2600, Shimadzu, Tokyo, Japan). The

171 film strips were placed into a spectrophotometer cell and recorded from 200 to 800 nm

172 (Mahmood Alizadeh-Sani, Tavassoli, McClements, & Hamishehkar, 2021). Air was

173 used as a blank sample. The transparency of the films was then calculated as follows:

174 $$\text{Transparency} = \frac{\log T_{600}}{D} \qquad (2)$$

175 where T_{600} was the optical transmittance of films at 600 nm (cm^{-1}) and D was the

176 thickness (mm) of films.

2.6. Physicochemical characterization of multifunctional films

2.6.1. Thickness, moisture content (MC), and water-solubility (WS)

179 The thickness was determined by measuring five random locations on a film. And

180 the MC and WS were determined according to the previous report (Zhang et al., 2021).

181 Firstly, the films were weighed and then dried in an oven (105°C for 24 h) to constant

182 weight. Secondly, the dried films were immersed in distilled water at 25°C for 24 h.

183 Finally, the surface water was removed from the films by filter paper and dried in an

184 oven at 105°C 24 h. The MC and WS of the films were calculated as follows:

185 $\quad$ MC (%) $= \frac{m_0 - m}{m_0} \times 100$ $\qquad$ (3)

186 $\quad$ WS (%) $= \frac{m - m_1}{m} \times 100$ $\qquad$ (4)

187 where m_0 was the weight of films before drying (g). m was the weight of films after

188 drying (g). m_1 was the drying weight of the films after immersing in water (g).

2.6.2. Mechanical properties and thermal stability (TGA)

190 $\qquad$ Tensile strength (TS) and elongation at break (EB) were measured with a texture

191 analyzer (Universal TA, Shanghai Tengba Instrument Technology Co., Ltd, China). The

192 mechanical properties of the film (1 cm $\times$ 4 cm) were tested at a constant speed of 10

193 mm/s with an initial gap separation of 20 mm.

194 $\qquad$ The thermal stability of the films was measured using a thermogravimetric

195 analyzer Mettler Toledo STARe System TGA2, Mettler Toledo Co, Switzerland). The

196 film samples were placed in a pan and scanned at a heating rate of 10 °C/min at a

197 temperature range of 30-600°C under a nitrogen atmosphere.

2.6.3. Water vapor permeability (WVP) and water contact angle

199 $\qquad$ The WVP was measured according to the previous report with some modifications

200 (Chen, et al., 2016). Each film was sealed on the top of a permeability cup (35 mm inner

201 diameter and 39 mm depth) filled with anhydrous calcium chloride. Each cup was

202 weighed periodically every 2 h for 2 d in an incubator with 75% RH at 25°C. The water

203 vapor permeability was calculated as follows:

204 $\quad$ WVP $= \frac{\Delta W \cdot D}{\Delta t \cdot S \cdot \Delta p}$ $\qquad$ (5)

205 where WVP was in g/Pa·h·m, ΔW is the gained weight of the cup (g), Δt is the time of

11

206 weight change (h), S was the exposed area of the films (m^2), D was the mean thickness

207 of samples (m), and Δp was the difference in partial water vapor pressure between the

208 two sides of films (Pa).

209 The water contact angle measurements were performed using an optical contact

210 angle analyzer (OSA200-T, New boundary Scientific Instrument Co. Ltd., Zhejiang,

211 China). A drop of ultrapure water (10 μL) was firstly placed on the surface of the films.

212 The image of the drop was then taken by a high-speed video camera, and the contact

213 angle was determined using the software after 5 s of the droplet deposition.

214 2.6.4. Scanning electron microscopy (SEM)

215 The film was immersed in liquid nitrogen to break, and the cross-section was

216 exposed. Afterward, the films were placed on the specimen holder, which was sputtered

217 by gold in a sputter coater. The films' morphology was examined by scanning electron

218 microscopy (SU-8010, HITACHI, Tokyo, Japan) at an accelerating voltage of 3 kV.

219 2.6.5. Fourier transform infrared (FT-IR) spectroscopy

220 The FT-IR spectra of the films were obtained using the attenuated total reflectance

221 Fourier Transform Infrared spectrometer (Vertex 670, Agilent Technologies, Santa

222 Clara, CA, USA) in the range of 4000 to 400 cm^{-1}. Each sample spectrum was collected

223 with 32 scans and 4 cm^{-1} resolution.

224 2.6.6. X-ray diffraction (XRD)

225 The crystal phase of the films was analyzed by an X-ray diffractometer (Bruker

226 D8 Advance, Karlsruhe, Germany) equipped with Cu Kα radiation (40 kV, 30 mA). The

227   XRD patterns of films were scanned from 5-50° (2θ) at 2°/min speed.

228   2.7. Functional characterization of multifunctional films

229   2.7.1. Acid gas sensitivity test

230   The films (2 cm diameters) were held above an acetic acid solution in a petri dish

231   at 25°C for 30 min to expose the films to acid gas. The acid gas response of the films

232   was captured and recorded by the digital camera at every 5 min intervals in 30 min.

233   2.7.2. Thyme oil release in food simulants

234   The release of TO was measured using different kinds of food simulant solutions

235   (20 mL, water, 10% (v/v), 50% (v/v), and 95% (v/v) alcohol for simulating aqueous,

236   alcoholic, and oil-in-water emulsions, and fatty food, respectively) (Lee, Kim, & Park,

237   2018). Briefly, the films (2 cm × 2 cm) were immersed in 20 mL of simulant, which

238   was stored at 37°C with 150 r/min. At appropriate intervals, the simulated solutions (1

239   mL) were collected and measured the absorbance at 274 nm using a UV-vis

240   spectrophotometer (UV-2600, Shimadzu, Tokyo, Japan).

241   2.7.3. Antioxidant quenching activity

242   The antioxidant activities of films were evaluated by DPPH and ABTS$^+$ radical

243   scavenging methods (Roy & Rhim, 2021c). The film samples were mixed with DPPH

244   and ABTS assay solution in the dark for 1 h at room temperature and measured the

245   absorbance at 517 nm and 734 nm using a UV-vis spectrophotometer (UV-2600,

246   Shimadzu, Tokyo, Japan). The radical scavenging ability was calculated by the

247   following equation listed as follows:

248    $$\text{Radical scavenging activity (\%)} = \left(1 - \frac{A}{A_0}\right) \times 100 \qquad (6)$$

249   where A and A_0 were the absorbances of the solutions treated with and without films,

250   respectively.

2.7.4. Antibacterial activity

252   A total viable colony count method was used to determine the antibacterial assay

253   of films against foodborne pathogenic bacteria *E. coli* and *S. aureus* according to the

254   previous reports with some modifications (Roy & Rhim, 2021b; Zhao et al., 2020).

255   Firstly, the films (2 cm × 2 cm) were added into the liquid medium which were

256   inoculated microorganisms (about 10^5 CFU/mL). All samples were incubated at 37℃

257   for 24 h with agitation at 100 rpm, and the resulting curves were constructed by

258   counting the total number of viable colonies by a plate count method. Specifically,

259   appropriate amount of microbial suspension was removed at predetermined time

260   intervals (0, 2, 4, 8, 12, 18 and 24 h), plated on agar plates after appropriate dilution to

261   determine the viable colony count.

2.8. Application of the films to milk preservation freshness monitoring

263   The actual functional effect of the films was evaluated by exploring the abilities

264   to indicate milk quality during storage (Gao et al., 2022). The films were adhered to the

265   bottle wall and soaked into 5 mL milk at 25℃ for storage. The pH and acidity of milk

266   were measured at different time points, and the films were taken out and wiped on the

267   surface to determine the color parameters. The acidity (°T) is expressed in the amount

268   of 0.1 mol/L sodium hydroxide consumed to neutralize 100 mL of milk, which was

269   determined using the acid-base titration method as the previous report with some

270   modifications (Gao et al., 2022).

2.9. Statistical analysis

272   All the experiments were performed in triplicate and expressed as the form of

273   mean ± standard deviation. The statistical tests were analyzed by SPSS software

274   (version 25.0, IBM; Armonk, N. Y, USA). All statistical data were evaluated by

275   ANOVA, and significance was defined as $P < 0.05$.

3. Results and discussion

3.1. Characterization of BOA solutions at different pH

278   The BOA solutions changed color from red to pink (pH 1.0-4.0) and pink to violet

279   (pH 4.0-10.0), as well as a sudden color change from violet to yellow (pH 10.0-14.0)

280   (**Fig. 2A**). These color changes were associated with pH-dependent alterations in the

281   anthocyanin molecular structure, consistent with the observed UV-vis spectra of BOA

282   solutions (**Fig. 2C**). With the increasing pH value, the maximum absorption wavelength

283   of BOA shifted from 521 nm to 580 nm, which was similar to previous reports (Chen,

284   Zhang, Bhandari, & Yang, 2020; Kim et al., 2022). These results might be attributed to

285   the reversible structural changes of anthocyanin from acidic to alkaline aqueous

286   medium (**Fig. 2B**): flavylium cation (pH < 4); carbinol pseudo base (pH 4-5);

287   quinonoidal anhydro base (pH 5-7); anionic quinonoidal base (pH 7-10) and chalcone

288   (pH > 10) (Mahmood Alizadeh-Sani et al., 2021). The apparent pH-dependent color

289 variation suggested that BOA was a suitable choice for developing intelligent

290 packaging.

3.2. Physicochemical characterization of multifunctional films

3.2.1. Appearances and optical properties of films

293   The CS/GA film was neat and transparent, while the E-CS/GA film changed

294 yellowish slightly with emulsion, and the BOA-added films were dark green (**Table 1**).

295 Correspondingly, L^* value and a^* value decreased significantly with the addition of

296 anthocyanin. Moreover, the transparency of the films decreased with the addition of the

297 emulsion, which might be due to the emulsion droplets scattered light in the films (Chen

298 et al., 2016). It should be noted that in the BOA addition films, the primary color of

299 anthocyanin was purple-red, but it turned green due to the slight alkalinity of the

300 chitosan/gum Arabic mixture. This phenomenon was similar to previous studies on

301 anthocyanin-chitosan, gelatin/agar, and gelatin/carrageenan films (Kim et al., 2022;

302 Yong, Wang, Zhang, et al., 2019; Roy & Rhim, 2020).

303   Compared with CS/GA film, the A-CS/GA film had stronger light barrier

304 properties, whose transmittance decreased by about 20% (**Fig. 3A**). A possible

305 explanation was that the anthocyanin was able to absorb both ultraviolet and visible

306 radiation (Yong, Wang, Bai, et al., 2019). The emulsion further reduced the

307 transmittance by more than 90% in the ultraviolet region at 200-400 nm. These results

308 could be explained by the dispersion of emulsion droplets in the films, blocking the

309 optical path or scattering light (Roy & Rhim, 2021b).

310 **3.2.2. Thickness, moisture content and water solubility of films**

311   The thickness of multifunctional films ranged from 34.35 to 44.2 μm (**Table 1**).

312 The addition of emulsion increased the film thickness obviously, which might be due

313 to more substances remaining in the films after dehydration (Sani et al., 2021). The

314 incorporation of anthocyanin had no significant effect on the films' moisture content

315 and water solubility (P > 0.05). However, with the addition of emulsion, these two

316 properties decreased obviously. There might be two reasons for these results: (i) The

317 strong hydrophobicity of essential oil further hindered the contact between the film

318 matrix and water (Zhang et al., 2021). (ii) The amino and hydroxyl groups of chitosan

319 interacted with anthocyanin, which reduced the accessibility of free -OH groups and

320 affected the ability to absorb water (Yong, Wang, Zhang, et al., 2019).

321 **3.2.3. Water vapor permeability and water contact angle of films**

322   The incorporation of BOA increased the water vapor transmittance slightly (**Fig.**

323 **3B**). After adding the emulsion, the water vapor barrier property was enhanced

324 obviously, which might be due to the strong hydrophobic essential oil intercepting most

325 of the water and increasing the tortuous path of water molecules through the films

326 (Zhang et al., 2022). The water vapor transmittance of 1A-E-CS/GA films was further

327 reduced to 5.78×10^{-11} $g \cdot m^{-1} \cdot h^{-1} \cdot Pa^{-1}$, which two aspects could explain: (i) A small

328 amount of anthocyanin interacted with the film matrix and acted as a bridge between

329 among substrate chains, forming a dense network (Yong, Wang, Bai, et al., 2019). (ii)

330 A large amount of aromatic ring in anthocyanin skeleton structure hindered the internal

331 network of the films and reduced the affinity for water molecules (Chen et al., 2021;

332 Wang et al., 2019). In contrast, a higher amount of anthocyanin (3A-E-CS/GA) might

333 lead to a decrease in the density of films (**Fig. 4**), thereby increasing the water vapor

334 permeability (Yong, Wang, Zhang, et al., 2019). Compared with previous relevant

335 studies which added anthocyanins or essential oil to the biopolymer (such as chitosan,

336 gum, κ-carrageenan, or cellulose) films, our multifunctional film had better water

337 resistance, which was conducive to protecting the excessive loss of food moisture

338 during storage (Rosenbloom, Wang, & Zhao, 2020; Wang, Zhang, & Zhang, 2022; Yong,

339 Liu, Kan, & Liu, 2022).

340 Generally, the water contact angle at 90° is usually defined as the critical point for

341 determining hydrophilicity or hydrophobicity (Zhang et al., 2022). The water contact

342 angle images and values of films are reported in **Fig. 3C**. The contact angle of CS/GA

343 films was 81.83°, and the addition of many anthocyanins reduced the contact angle by

344 74.64°. These results were due to a great number of free hydroxyl groups in the film

345 matrix and the high hydrophilicity of anthocyanin (Liu et al., 2022). With the

346 incorporation of emulsion, the films' contact angle increased obviously to 96.7°, which

347 could be attributed to the increase of hydrophobic components (thyme oil) and surface

348 roughness of the films (Liu et al., 2022). It is important to note that a small amount of

349 anthocyanin addition enhanced the hydrophobicity of the films, which was similar to

350 the results of WVP, which could be attributed to the aromatic ring of anthocyanin

351 structure and the interaction between anthocyanin and film matrix (Wang et al., 2019).

3.2.4. Mechanical property and structures of films

352

353   The mechanical strength of CS/GA films was poor, where the tensile strength (TS)

354   was 20.45 MPa, and the elongation at break (EB) was 40.78% (**Table 1**). The addition

355   of anthocyanin enhanced the mechanical strength and flexibility of the films, but there

356   was no significant change ($P > 0.05$). The addition of emulsion improved the films'

357   mechanical properties significantly, which could be due to the interaction between

358   emulsion droplets and the film matrix, producing a cross-linking agent effect (Haghighi

359   et al., 2019; Ojagh, Rezaei, Razavi, & Hosseini, 2010). In addition, the TS of emulsion

360   films decreased from 34.87 to 31.89 MPa, while the EB increased from 61.26 to 76.1%

361   with the increase of anthocyanin content. This phenomenon could be due to the strong

362   plasticization of anthocyanin, which destroyed the secondary bonds and improved the

363   fluidity of polymer molecule chains in the films (Kim et al., 2022). Meanwhile, the

364   rearrangement of biopolymer produced uneven network and discontinuous pore

365   structure in the films (Haghighi et al., 2019), which also led to a decrease in tensile

366   strength, as shown by the microstructure of the films (**Fig. 4**). Previous researchers

367   added cinnamon and clove essential oil to chitosan-gum Arabic film. The maximum TS

368   of the composite film was 24.06 MPa and the maximum EB was 41.03% (Xu et al.,

369   2019). Compared with it, our multifunctional film had stronger mechanical strength,

370   which might be more suitable for a variety of food packaging. It can be observed that

371   CS/GA films had compact and smooth micro-morphology, which indicated a good

372   interaction and compatibility between gum Arabic and chitosan matrix. The addition of

373 BOA made the film cross-section smoother. It was related to the plasticizing effect of

374 anthocyanin (Wu et al., 2019). When the emulsion was added to the film matrix, the

375 film surface was rough, and the cross-section became porous, similar to previous

376 studies (Kong et al., 2020; Liu, Shen, Yang, & Lin, 2021). The existence of pores was

377 mainly due to the essential oil in the film matrix volatilizing and migrating to the top

378 during the casting process (Liu et al., 2022; Xu et al., 2020; Zhang et al., 2021).

379 3.2.5. The molecular interaction and crystallinity of films

380 The intermolecular interaction of the films was further analyzed by FT-IR and

381 XRD. The molecular characteristics of BOA and the multifunctional films observed

382 through FT-IR are presented in **Fig. 5A**. The FT-IR spectrum of free anthocyanins

383 showed that the characteristic band at 1639 cm^{-1} was caused by the benzene skeleton

384 vibration in anthocyanins (Wu et al., 2019), and the peak at 2932 cm^{-1} was assigned to

385 the stretching vibration of -CH, $-CH_2$, and $-CH_3$. The board and drastic band at around

386 3369 cm^{-1} was attributed to the stretching vibration of the -OH and hydrogen bond.

387 After anthocyanins were added into the films, the characteristic band at 1639 cm^{-1} was

388 masked, indicating that the films immobilized the anthocyanins and had a certain

389 protective effect. Meanwhile, the absorption peak near 3369 cm^{-1} attributed to the

390 overlapping stretching vibration of -OH becomes wider, indicating that a hydrogen

391 bond was formed between BOA and the film matrix (Chen et al., 2021). The peaks at

392 1563 cm^{-1} and 1409 cm^{-1} of CS/GA film, which were caused by the carboxy group

393 (overlapped with N-H bending) and $-CH_2COOH$ group of chitosan, shifted to 1574 cm^{-}

394   ^{1} and 1411 cm^{-1} for the A-CS/GA film, and to 1565 cm^{-1} and 1414 cm^{-1} for the 3A-E-

395   CS/GA. This band shifting might be attributed to aromatic ring stretching due to the

396   interaction between the anthocyanin and the glycosylated polymers matrix (Sohany,

397   Tawakkal, Ariffin, Shah, & Yusof, 2021). The FT-IR results showed that no new

398   chemical bonds were formed during the film preparation, indicating that materials were

399   formed in a non-covalent cross-linking method (Wu et al., 2019). As a color indicator,

400   anthocyanins were anchored inside the film matrix by hydrogen bonds with electrostatic

401   interactions (Liang, Sun, Cao, Li, & Wang, 2019).

402   There was no obvious change in the position of the peaks, and no new peaks

403   appeared in the XRD patterns (**Fig. 5B**), indicating that the emulsions and BOA were

404   well dispersed in the film matrix (Huang, et al., 2019). Meanwhile, all films had similar

405   XRD patterns, which appeared with a single diffraction peak at 19.7°, while the

406   intensity was significantly different. The peak strength of the films increased slightly

407   with the addition of BOA, which might be due to the plasticization of anthocyanin and

408   the electrostatic interaction between the film matrix and BOA (Liang, Sun, Cao, Li, &

409   Wang, 2019). The addition of emulsion significantly increased the crystallinity of the

410   films, which indicated that there was a stronger interaction between the filler and the

411   matrix, and was conducive to the enhancement of the mechanical and barrier properties

412   of the films (Tavassoli, Sani, Khezerlou, Ehsani, & McClements, 2021).

413   **3.2.6. Thermal stability of films**

414   The weight loss of the film without emulsion was divided into three stages during

415 thermal degradation (**Fig. 5C and D**). The first stage was observed at 50-105℃,

416 attributed to the water vaporization. The second weight change was 130-230℃, caused

417 by glycerol decomposition (Ezati & Rhim, 2020). The third weight stage (230-320℃)

418 corresponded to the thermal depolymerization and decomposition of the film matrix

419 (Yong, Wang, Bai, et al., 2019). The 3A-E-CS/GA film took the fourth stage of

420 weightlessness at 400-450℃, which was related to the incorporation of emulsion,

421 suggesting the loss of high-temperature stable components (Liu et al., 2021). Moreover,

422 when anthocyanin and emulsion were added to the films, the weight loss of the first and

423 the second stages decreased significantly, indicating that the interaction between

424 anthocyanin and glycerol could reduce the glycerol decomposition rate (Wang et al.,

425 2019). A previous study incorporated blueberry anthocyanins into ovalbumin-cellulose

426 film and found the main degradation peaks of the films moved to higher temperatures

427 with the addition of anthocyanins, which was similar to our results (Liu, et al., 2022).

428 Meanwhile, the emulsion droplets could reduce the moisture content in the films and

429 interact with the film matrix, thus enhancing the thermal stability of the films (Xu et al.,

430 2019).

431 **3.3. Color response of films to pH and volatile acid**

432   The color response performance of multifunctional films at different pH is shown

433 in **Table 2**. CS/GA film was always gray-white, and its color parameters had no

434 apparent change. The E-CS/GA film's color was yellowed by the addition of emulsion,

435 while it still did not have pH color responsiveness. In contrast, when the pH changed

436   from 3.0 to 13.0, the films added with BOA exhibited a significant color change from

437   pink to green. Meanwhile, with the pH increase, the $a*$ decreased, while the $b*$

438   increased. In addition, the film color deepened accordingly with the increase of

439   anthocyanin content. These phenomena were due to the structural transformation of

440   anthocyanins under different acid-base conditions, which were similar to previous

441   research on the packaging films containing anthocyanins from other sources (Wu et al.,

442   2019; Alizadeh Sani et al., 2022; Chen et al., 2021). In addition, all anthocyanin films'

443    $\varDelta E$ values were more than 5.0, indicating that the chromatic aberration was easy to be

444   observed by the naked eyes (Chen et al., 2021). In addition, the films' pH color

445   sensitivity had excellent stability (**Table S1**). After storage in indoor conditions for 3

446   months, the films still had a sensitive color response to pH change, whose color changed

447   from red to green and then to yellow with the increase of pH. In particular, the $\varDelta E$ values

448   of the 3A-E-CS/GA film could still be maintained above 15, indicating that the color

449   change was easy to recognize by the naked eyes. These results suggested that the films

450   had great color stability, which had a specific protective effect on anthocyanins.

451   The color sensitivity of films to acid gas is presented in **Fig. S3**. When anthocyanin

452   films were exposed to volatile acids, their color changed significantly from yellow-

453   green to red over time. The films with high anthocyanin content showed noticeable

454   color changes, from green to yellow-green after 10 min and pink after 15 min. These

455   results indicated that this multifunctional film had the potential to monitor food

456   freshness in real time.

3.4. Release profiles of thyme oil and anthocyanin in films

457

458   There were mainly two steps involved in the release behavior of essential oil from

459   films. Firstly, the liquid molecule penetrated the polymer matrix, causing the polymer

460   network structure to expand and weaken. Afterward, essential oil molecules were

461   diffused from inside the films to the stimulants until reaching the thermodynamic

462   equilibrium (Zhang et al., 2021). Depending on the type of food stimulants, thyme oil

463   was released at varying rates. In most cases, the release rate was rapid at first but slowed

464   down to equilibrium after 12 h. The release effect of thyme oil was the worst in water,

465   which only reached 19.16 $\mu g/mm^2$ (**Fig. 6A**). Thyme oil was a hydrophobic substance

466   that was released faster in alcohol solutions than in water. However, the release rate was

467   related to the concentration of alcohol. The release rate in 50% alcohol was higher than

468   95%, and the release rate in 10% alcohol was the lowest. The low release rate in 95%

469   alcohol solution might result from the slight swelling of biopolymer films under high

470   alcohol conditions (Roy & Rhim, 2020).

471   The anthocyanin was released the fastest in the 10% alcohol solution, followed by

472   water, 50% alcohol, and 95% alcohol solutions (**Fig. S2**), mainly due to the polarity of

473   water-soluble anthocyanin pigment. The release rate was affected by the type and

474   polarity of the food simulant and the swelling of the film (Alizadeh-Sani, et al., 2021).

475   This result was similar to the previously reported results of the release of other

476   anthocyanins from biopolymer film into food simulants (Alizadeh-Sani, Tavassoli,

477   McClements, & Hamishehkar, 2021; Alizadeh Sani, Tavassoli, Salim, Azizi-lalabadi,

478   & McClements, 2022).

3.5. Antioxidant and antibacterial activity of films

480   The oxidation resistance of films was evaluated by ABTS and DPPH radical

481   scavenging activity, whose results are demonstrated in **Fig. 6B**. The CS/GA films had

482   a weak antioxidant capacity of 6.57%, which might be associated with the extent of the

483   hydroxyl group (C6) and amino group (C2) in chitosan (Xie, Xu, & Liu, 2001). The

484   addition of anthocyanin noticeably enhanced the antioxidant capacity of the films due

485   to many phenolic groups in the anthocyanin molecular structure (Alizadeh Sani et al.,

486   2022). At present, a lot of studies have reported that the incorporation of anthocyanin

487   improved the ABTS and DPPH scavenging ability of films, which was consistent with

488   our research results (Fernández-Marín et al., 2022; Alizadeh Sani, et al., 2022; Wang,

489   et al., 2022). The thyme oil emulsion further improved the free radical scavenging

490   ability of the films to more than 85%, which could be mainly because the essential oil

491   was an excellent antioxidant and acted in conjunction with anthocyanins (Fernández-

492   Marín et al., 2022). It should be noted that the A-CS/GA films' radical scavenging

493   ability to ABTS was significantly higher than that to DPPH, while it was the opposite

494   in emulsion films. This phenomenon might be associated with the different solubility

495   of anthocyanins and essential oil (Roy & Rhim, 2021c).

496   The dynamic antimicrobial activity was evaluated against two model bacteria (*E.*

497   *coli* and *S. aureus*), which is shown in **Fig. 6C and D**. The microorganisms in the

498   control group grew rapidly, and the bacterial number reached 10^9 CFU/mL in 12 h. The

499   CS/GA films showed weak antibacterial activity, while the bacteria also proliferated to

500   10^7 CFU/mL in 24 h, which was attributed to the interaction between the positive charge

501   with chitosan and negatively charged cell membrane, leading to membrane damage and

502   cell content leakage (Mahmood Alizadeh-Sani et al., 2021). The further incorporation

503   of BOA enhanced the antibacterial potency of the films due to the polyphenol structure

504   of anthocyanin (Sani et al., 2021). The antibacterial properties of the emulsion films

505   increased obviously, which could be due to the excellent antibacterial activity of thyme

506   oil and the slow-release effect of the emulsion (Zhang et al., 2021). In contrast, the

507   addition of thyme oil emulsion and higher concentration anthocyanin films completely

508   prevented the bacterial growth after 4 h, indicating that the two played an antibacterial

509   role together to further improve the antibacterial property of the films, which was

510   similar to the previous report about the bioactive films integrated with cinnamon oil

511   and rutin (Roy & Rhim, 2021c). It was noteworthy that the films' inhibition ability on

512   *S. aureus* was greater than that of *E. coli*, which might be related to the discrepancy in

513   cell wall structure between the two bacteria (Zhang et al., 2019).

514   **3.6. Application of films in milk preservation and spoilage monitoring**

515   Milk usually tends to spoilage and becomes sour during storage. Therefore, we

516   investigated the stability and applicability of multifunctional films in milk preservation

517   and freshness monitoring (**Fig. 7A**). The initial pH and acidity of milk were 6.6 and

518   16.8°T, respectively. With the increase of storage time, the pH of milk in the control

519   group decreased rapidly, and the acidity increased significantly. After 24 h, the acidity

520   in the control group reached 25°T and exceeded 40°T in 48 h, appearing the obvious

521   spoilage (**Fig. 7C and D**). The multifunctional films significantly slowed down the

522   rancidity process of milk, which made pH maintain above 6 and the acidity keep below

523   30°T within 48 h. Meanwhile, the films maintained the total number of colonies in milk

524   below 10^5 CFU/mL for 48 h, which showed an excellent antibacterial effect (**Fig. 7E**).

525   Some researchers constructed starch films containing carrot anthocyanins, which were

526   applied to the storage of milk. The results showed that the acidity of milk was 28°T and

527   the total number of colonies reached 10^7 after 48 h of storage (Moazami Goodarzi, et

528   al., 2020). This indicated that compared with previous studies, our multifunctional film

529   had a better preservative and fresh-keeping effect, which could prolong the shelf-life of

530   milk. In addition, the films containing BOA had the function of indicating milk

531   freshness (**Fig. 7B**). After 48 h, the microorganisms in the milk exceeded 10^7 CFU/mL,

532   indicating that the milk had deteriorated (Moazami Goodarzi, et al., 2020). At the same

533   time, the film color changed from green to red, and the *a** value also changed from -

534   3.84 to 3.06 (**Fig. 7F**). Meanwhile, the strong positive correlation between the total

535   number of colonies and chroma *a** (R^2 = 0.994) was depicted in (**Fig. S4**), and it was

536   estimated that an exponent model best matched the data. Moreover, the chroma *a** was

537   also correlated with the acid of milk and had a higher precision index (R^2 = 0.995).

538   These results indicated that we could recognize the freshness of milk from the change

539   of film color. Moreover, the *ΔE* value of 3A-E-CS/GA films always maintained above

540   20 (**Fig. 7G**), which was easy to observe with the naked eyes. Previous studies added

27

541 blueberry anthocyanin, purple and black eggplant anthocyanin, or shikonin to

542 biopolymer films to fabricate intelligent packaging for milk storage (Gao, et al., 2022;

543 Yong, et al., 2019; Roy & Rhim, 2020). Their results showed that the color of the film

544 changes from dark purple or dark blue to light purple or light blue, which might be

545 detrimental to consumers' visual discrimination. Compared with these studies, the

546 process from green to red was more obvious, which was more conducive to visual

547 observation. Therefore, these results indicated that our multifunctional films had

548 excellent application potential in prolonging the shelf-life of milk and monitoring milk

549 freshness.

550 **4. Conclusions**

551 In summary, novel multifunctional films based on chitosan/gum Arabic were

552 successfully fabricated by incorporating thyme oil emulsion and blood orange

553 anthocyanins. The addition of anthocyanin and emulsion improved the films' optical

554 properties, making them have excellent UV barrier properties. Anthocyanin could be

555 used as a plasticizer to improve the mechanical properties of the films, whose

556 elongation at break increased to 76.1%. The hydrophobicity of the essential oil

557 increased the barrier properties of the film, which made the films' water vapor

558 transmission rate decrease significantly. Meanwhile, the film color rested with the

559 environmental pH and acid gas content, which was attributed to the pH color

560 responsiveness of anthocyanin and could be potentially applied to monitor food

561 freshness. In addition, the multifunctional films had a slow-release effect on the

562 essential oil, giving them excellent antioxidant and dynamic antibacterial abilities. The

563 films effectively prolonged the shelf-life of milk, which could be reflected in inhibiting

564 the reproduction of spoilage bacteria and slowing down the rancidity phenomenon. The

565 films could also monitor milk spoilage in real-time by color changes (from yellow-

566 green to red) and had high visual recognition. This multifunctional packaging material

567 is promising to be further used in the food industry due to its excellent capacities for

568 food preservation and quality monitoring.

569 **Acknowledgments**

573 **References**

574 Alizadeh Sani, M., Tavassoli, M., Salim, S. A., Azizi-lalabadi, M., & McClements, D.

575   J. (2022). Development of green halochromic smart and active packaging

576   materials: TiO$_2$ nanoparticle- and anthocyanin-loaded gelatin/κ-carrageenan

577   films. *Food Hydrocolloids,* 124.

578 Alizadeh-Sani, M., Tavassoli, M., McClements, D. J., & Hamishehkar, H. (2021).

579   Multifunctional halochromic packaging materials: Saffron petal anthocyanin

580   loaded-chitosan nanofiber/methyl cellulose matrices. *Food Hydrocolloids,* 111.

581 Alizadeh-Sani, M., Tavassoli, M., Mohammadian, E., Ehsani, A., Khaniki, G. J.,

582   Priyadarshi, R., & Rhim, J. W. (2021). pH-responsive color indicator films

583   based on methylcellulose/chitosan nanofiber and barberry anthocyanins for

584   real-time monitoring of meat freshness. *International Journal of Biological*

585   *Macromolecules, 166*, 741-750.

586   Atta, O. M., Manan, S., Shahzad, A., Ul-Islam, M., Ullah, M. W., & Yang, G. (2022).

587   Biobased materials for active food packaging: A review. *Food Hydrocolloids,*

588   *125*.

589   Azman, N. H., Khairul, W. M., & Sarbon, N. M. (2022). A comprehensive review on

590   biocompatible film sensor containing natural extract: Active/intelligent food

591   packaging. *Food Control, 141*.

592   Becerril, R., Nerín, C., & Silva, F. (2021). Bring some colour to your package:

593   Freshness indicators based on anthocyanin extracts. *Trends in Food Science &*

594   *Technology, 111*, 495-505.

595   Carmona, L., Alquezar, B., Marques, V. V., & Pena, L. (2017). Anthocyanin

596   biosynthesis and accumulation in blood oranges during postharvest storage at

597   different low temperatures. *Food Chemistry, 237*, 7-14.

598   Chen, H., Hu, X., Chen, E., Wu, S., McClements, D. J., Liu, S., Li, B., & Li, Y. (2016).

599   Preparation, characterization, and properties of chitosan films with

600   cinnamaldehyde nanoemulsions. *Food Hydrocolloids, 61*, 662-671.

601   Chen, H.-z., Zhang, M., Bhandari, B., & Yang, C.-h. (2020). Novel pH-sensitive films

602   containing curcumin and anthocyanins to monitor fish freshness. *Food*

603   *Hydrocolloids, 100*.

604   Chen, M., Yan, T., Huang, J., Zhou, Y., & Hu, Y. (2021). Fabrication of halochromic

605   smart films by immobilizing red cabbage anthocyanins into chitosan/oxidized-

606   chitin nanocrystals composites for real-time hairtail and shrimp freshness

607   monitoring. *International Journal of Biological Macromolecules, 179*, 90-100.

608   Chen, W., Ma, S., Wang, Q., McClements, D. J., Liu, X., Ngai, T., & Liu, F. (2022).

609   Fortification of edible films with bioactive agents: a review of their formation,

610   properties, and application in food preservation. *Crit Rev Food Sci Nutr, 62*(18),

611   5029-5055.

612   Ezati, P., & Rhim, J.-W. (2020). pH-responsive chitosan-based film incorporated with

613   alizarin for intelligent packaging applications. *Food Hydrocolloids, 102*.

614   Fernández-Marín, R., Fernandes, S. C. M., Sánchez, M. Á. A., & Labidi, J. (2022).

615   Halochromic and antioxidant capacity of smart films of chitosan/chitin

616   nanocrystals with curcuma oil and anthocyanins. *Food Hydrocolloids, 123*.

617   Gao, R., Hu, H., Shi, T., Bao, Y., Sun, Q., Wang, L., Ren, Y., Jin, W., Yuan, L. (2022).

618   Incorporation of gelatin and Fe(2+) increases the pH-sensitivity of zein-

619   anthocyanin complex films used for milk spoilage detection. *Current Research*

620   *in Food Science, 5*, 677-686.

621   Guo, M., Zhang, L., He, Q., Arabi, S. A., Zhao, H., Chen, W., Ye, X., & Liu, D. (2020).

622   Synergistic antibacterial effects of ultrasound and thyme essential oils

623   nanoemulsion against *Escherichia coli O157:H7. Ultrasonics - Sonochemistry,*

624   66, 104988.

625   Habibi, F., Garcia-Pastor, M. E., Puente-Moreno, J., Garrido-Aunon, F., Serrano, M., &

626   Valero, D. (2022). Anthocyanin in blood oranges: a review on postharvest

627   approaches for its enhancement and preservation. *Critical Reviews in Food*

628   *Science and Nutrition*, 1-13.

629   Haghighi, H., Biard, S., Bigi, F., De Leo, R., Bedin, E., Pfeifer, F., Siesler, H.,

630   Licciardello, F., & Pulvirenti, A. (2019). Comprehensive characterization of

631   active chitosan-gelatin blend films enriched with different essential oils. *Food*

632   *Hydrocolloids,* 95, 33-42.

633   Huang, J., Hu, Z., Li, G., Hu, L., Chen, J., & Hu, Y. (2022). Make your packaging

634   colorful and multifunctional: The molecular interaction and properties

635   characterization of natural colorant-based films and their applications in food

636   industry. *Trends in Food Science & Technology, 124*, 259-277.

637   Huang, S., Xiong, Y., Zou, Y., Dong, Q., Ding, F., Liu, X., & Li, H. (2019). A novel

638   colorimetric indicator based on agar incorporated with Arnebia euchroma root

639   extracts for monitoring fish freshness. *Food Hydrocolloids, 90*, 198-205.

640   Kim, H.-J., Roy, S., & Rhim, J.-W. (2022). Gelatin/agar-based color-indicator film

641   integrated with Clitoria ternatea flower anthocyanin and zinc oxide

642   nanoparticles for monitoring freshness of shrimp. *Food Hydrocolloids,* 124.

643   Kong, R., Wang, J., Cheng, M., Lu, W., Chen, M., Zhang, R., & Wang, X. (2020).

644   Development and characterization of corn starch/PVA active films incorporated

645   with carvacrol nanoemulsions. *International Journal of Biological*

646   *Macromolecules,* 164, 1631-1639.

647   Lee, M. H., Kim, S. Y., & Park, H. J. (2018). Effect of halloysite nanoclay on the

648   physical, mechanical, and antioxidant properties of chitosan films incorporated

649   with clove essential oil. *Food Hydrocolloids, 84*, 58-67.

650   Liang, T., Sun, G., Cao, L., Li, J., & Wang, L. (2019). A pH and NH3 sensing intelligent

651   film based on Artemisia sphaerocephala Krasch. gum and red cabbage

652   anthocyanins anchored by carboxymethyl cellulose sodium added as a host

653   complex. *Food Hydrocolloids, 87*, 858-868.

654   Liu, J., Song, F., Chen, R., Deng, G., Chao, Y., Yang, Z., Wu, H., Bai, M., Zhang, P., &

655   Hu, Y. (2022). Effect of cellulose nanocrystal-stabilized cinnamon essential oil

656   Pickering emulsions on structure and properties of chitosan composite films.

657   *Carbohydrate Polymers,* 275, 118704.

658   Liu, L., Wu, W., Zheng, L., Yu, J., Sun, P., & Shao, P. (2022). Intelligent packaging

659   films incorporated with anthocyanins-loaded ovalbumin-carboxymethyl

660   cellulose nanocomplexes for food freshness monitoring. *Food Chemistry, 387*,

661   132908.

662   Liu, L., Zhang, J., Zou, X., Arslan, M., Shi, J., Zhai, X., Xiao, J., Wang, X., Huang, X.,

663   Li, Z., & Li, Y. (2022). A high-stable and sensitive colorimetric nanofiber sensor

664   based on PCL incorporating anthocyanins for shrimp freshness. *Food Chemistry,*

665   377, 131909.

666   Liu, Z., Shen, R., Yang, X., & Lin, D. (2021). Characterization of a novel konjac

667   glucomannan film incorporated with Pickering emulsions: Effect of the

668   emulsion particle sizes. *International Journal of Biological Macromolecules,*

669   179, 377-387.

670   Moazami Goodarzi, M., Moradi, M., Tajik, H., Forough, M., Ezati, P., & Kuswandi, B.

671   (2020). Development of an easy-to-use colorimetric pH label with starch and

672   carrot anthocyanins for milk shelf life assessment. *International Journal of*

673   *Biological Macromolecules, 153*, 240-247.

674   Mohammadian, E., Alizadeh-Sani, M., & Jafari, S. M. (2020). Smart monitoring of

675   gas/temperature changes within food packaging based on natural colorants.

676   *Comprehensive Reviews in Food Science and Food Safety,* 19(6), 2885-2931.

677   Mukurumbira, A. R., Shellie, R. A., Keast, R., Palombo, E. A., & Jadhav, S. R. (2022).

678   Encapsulation of essential oils and their application in antimicrobial active

679   packaging. *Food Control, 136*.

680   Neves, D., Andrade, P. B., Videira, R. A., de Freitas, V., & Cruz, L. (2022). Berry

681   anthocyanin-based films in smart food packaging: A mini-review. *Food*

682   *Hydrocolloids, 133*.

683   Ojagh, S. M., Rezaei, M., Razavi, S. H., & Hosseini, S. M. H. (2010). Development

684   and evaluation of a novel biodegradable film made from chitosan and cinnamon

685   essential oil with low affinity toward water. *Food Chemistry,* 122(1), 161-166.

686   Pirsa, S., Sani, I. K., & Mirtalebi, S. S. (2022). Nano-biocomposite based color sensors:

687   Investigation of structure, function, and applications in intelligent food

688   packaging. *Food Packaging and Shelf Life, 31*.

689   Rosenbloom, R. A., Wang, W., & Zhao, Y. (2020). Delaying ripening of 'Bartlett' pears

690   (Pyrus communis) during long-term simulated industrial cold storage:

691   Mechanisms and validation of chitosan coatings with cellulose nanocrystals

692   Pickering emulsions. *LWT - Food Science and Technology, 122*.

693   Roy, S., & Rhim, J. W. (2020). Preparation of Gelatin/Carrageenan-Based Color-

694   Indicator Film Integrated with Shikonin and Propolis for Smart Food Packaging

695   Applications. *ACS Applied Bio Materials,* 4(1), 770-779.

696   Roy, S., & Rhim, J. W. (2021a). Anthocyanin food colorant and its application in pH-

697   responsive color change indicator films. *Critical Reviews in Food Science and*

698   *Nutrition, 61*(14), 2297-2325.

699   Roy, S., & Rhim, J. W. (2021b). Carrageenan/agar-based functional film integrated with

700   zinc sulfide nanoparticles and Pickering emulsion of tea tree essential oil for

701   active   packaging   applications. *International   Journal   of   Biological*

702   *Macromolecules,* 193(Pt B), 2038-2046.

703   Roy, S., & Rhim, J. W. (2021c). Fabrication of bioactive binary composite film based

704   on gelatin/chitosan incorporated with cinnamon essential oil and rutin. *Colloids*

705   *Surf B Biointerfaces,* 204, 111830.

706   Sani, M. A., Tavassoli, M., Hamishehkar, H., & McClements, D. J. (2021).

707   Carbohydrate-based films containing pH-sensitive red barberry anthocyanins:

708   Application as biodegradable smart food packaging materials. *Carbohydrate*

709   *Polymers,* 255, 117488.

710   Sohany, M., Tawakkal, I., Ariffin, S. H., Shah, N., & Yusof, Y. A. (2021).

711   Characterization of Anthocyanin Associated Purple Sweet Potato Starch and

712   Peel-Based pH Indicator Films. *Foods, 10*(9).

713   Tavassoli, M., Sani, M. A., Khezerlou, A., Ehsani, A., & McClements, D. J. (2021).

714   Multifunctional nanocomposite active packaging materials: Immobilization of

715   quercetin, lactoferrin, and chitosan nanofiber particles in gelatin films. *Food*

716   *Hydrocolloids, 118.*

717   Wang, X., Yong, H., Gao, L., Li, L., Jin, M., & Liu, J. (2019). Preparation and

718   characterization of antioxidant and pH-sensitive films based on chitosan and

719   black soybean seed coat extract. *Food Hydrocolloids,* 89, 56-66.

720   Wang, Y., Zhang, J., & Zhang, L. (2022). An active and pH-responsive film developed

721   by sodium carboxymethyl cellulose/polyvinyl alcohol doped with rose

722   anthocyanin extracts. *Food Chemistry, 373*(Pt B), 131367.

723   Wu, C., Sun, J., Zheng, P., Kang, X., Chen, M., Li, Y., Ge, Y., Hu, Y., & Pang, J. (2019).

724   Preparation of an intelligent film based on chitosan/oxidized chitin nanocrystals

725   incorporating black rice bran anthocyanins for seafood spoilage monitoring.

726   *Carbohydrate Polymers,* 222, 115006.

727   Xie, W. M., Xu, P. X., & Liu, Q. (2001). Antioxidant activity of water-soluble chitosan

728   derivatives. *Bioorganic & Medicinal Chemistry Letters,* 11(13), 1699-1701.

729   Xu, T., Gao, C., Feng, X., Huang, M., Yang, Y., Shen, X., & Tang, X. (2019). Cinnamon

730　　and clove essential oils to improve physical, thermal and antimicrobial

731　　properties of chitosan-gum arabic polyelectrolyte complexed films.

732　　*Carbohydrate Polymers,* 217, 116-125.

733　Xu, Y., Chu, Y., Feng, X., Gao, C., Wu, D., Cheng, W., Meng, L., Zhang, Y., & Tang,

734　　X. (2020). Effects of zein stabilized clove essential oil Pickering emulsion on

735　　the structure and properties of chitosan-based edible films. *International*

736　　*Journal of Biological Macromolecules,* 156, 111-119.

737　Yang, Z., He, Q., Ismail, B. B., Hu, Y., & Guo, M. (2022). Ultrasonication induced

738　　nano-emulsification of thyme essential oil: Optimization and antibacterial

739　　mechanism against Escherichia coli. *Food Control,* 133.

740　Yong, H., Liu, J., Kan, J., & Liu, J. (2022). Active/intelligent packaging films developed

741　　by immobilizing anthocyanins from purple sweetpotato and purple cabbage in

742　　locust bean gum, chitosan and kappa-carrageenan-based matrices. *International*

743　　*Journal of Biological Macromolecules, 211*, 238-248.

744　Yong, H., Wang, X., Bai, R., Miao, Z., Zhang, X., & Liu, J. (2019). Development of

745　　antioxidant and intelligent pH-sensing packaging films by incorporating purple-

746　　fleshed sweet potato extract into chitosan matrix. *Food Hydrocolloids,* 90, 216-

747　　224.

748　Yong, H., Wang, X., Zhang, X., Liu, Y., Qin, Y., & Liu, J. (2019). Effects of

749　　anthocyanin-rich purple and black eggplant extracts on the physical, antioxidant

750　　and pH-sensitive properties of chitosan film. *Food Hydrocolloids,* 94, 93-104.

751 Yun, D., & Liu, J. (2022). Recent advances on the development of food packaging films

752   based on citrus processing wastes: A review. *Journal of Agriculture and Food*

753   *Research, 9.*

754 Zhang, J., Huang, X., Zhang, J., Liu, L., Shi, J., Muhammad, A., Zhai, X., Zou, X., Xiao,

755   J., Li, Z., & Shen, T. (2022). Development of nanofiber indicator with high

756   sensitivity for pork preservation and freshness monitoring. *Food Chemistry,* 381,

757   132224.

758 Zhang, S., He, Z., Xu, F., Cheng, Y., Waterhouse, G. I. N., Sun-Waterhouse, D., & Wu,

759   P. (2022). Enhancing the performance of konjac glucomannan films through

760   incorporating zein–pectin nanoparticle-stabilized oregano essential oil

761   Pickering emulsions. *Food Hydrocolloids,* 124.

762 Zhang, W., Jiang, H., Rhim, J. W., Cao, J., & Jiang, W. (2022). Effective strategies of

763   sustained release and retention enhancement of essential oils in active food

764   packaging films/coatings. *Food Chemistry, 367*, 130671.

765 Zhang, X., Guo, M., Ismail, B. B., He, Q., Jin, T. Z., & Liu, D. (2021). Informative and

766   corrective responsive packaging: Advances in farm-to-fork monitoring and

767   remediation of food quality and safety. *Compr Rev Food Sci Food Saf, 20*(5),

768   5258-5282.

769 Zhang, X., Liu, D., Jin, T. Z., Chen, W., He, Q., Zou, Z., Zhao, H., Ye, X., & Guo, M.

770   (2021). Preparation and characterization of gellan gum-chitosan polyelectrolyte

771   complex films with the incorporation of thyme essential oil nanoemulsion. *Food*

772   *Hydrocolloids,* 114.

773   Zhang, X., Liu, Y., Yong, H., Qin, Y., Liu, J., & Liu, J. (2019). Development of

774   multifunctional food packaging films based on chitosan, TiO2 nanoparticles and

775   anthocyanin-rich black plum peel extract. *Food Hydrocolloids,* 94, 80-92.

776   Zhao, R., Song, R., Sun, G., Liu, S., Li, B., Cao, Y., & Li, Y. (2020). Cutoff Ostwald

777   ripening stability of eugenol-in-water emulsion by co-stabilization method and

778   antibacterial activity evaluation. *Food Hydrocolloids,* 107.

779   Zhao, R., Zhang, Y., Chen, H., Song, R., & Li, Y. (2022). Performance of eugenol

780   emulsion/chitosan edible coating and application in fresh meat preservation.

781   *Journal of Food Processing and Preservation,* 106407.
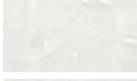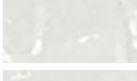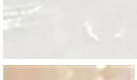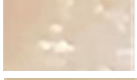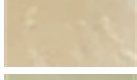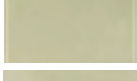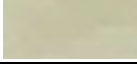
Table 1 Physico-mechanical, colorimetry and functional properties of the multifunctional packaging films (Different letters indicate significant difference, P < 0.05).
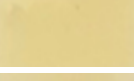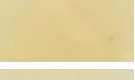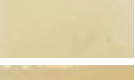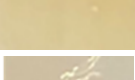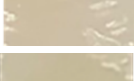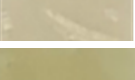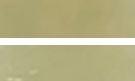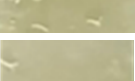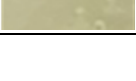
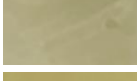| Parameters	CS/GA	A-CS/GA	E-CS/GA	1A-E-CS/GA	3A-E-CS/GA
Appearance					
Thickness (μm)	34.35 ± 1.28^a	36.15 ± 2.20^a	43.45 ± 1.03^b	43.85 ± 1.63^b	44.2 ± 4.88^b
Moisture content (%)	27.50 ± 0.49^c	26.98 ± 0.78^c	21.63 ± 0.84^b	21.25 ± 0.48^b	19.41 ± 0.75^a
Water solubility (%)	26.79 ± 1.04^b	28.63 ± 1.86^b	19.83 ± 00.74^a	20.61 ± 0.69^a	21.71 ± 0.51^a
Transparency (logT600/mm)	56.61 ± 0.05^e	49.84 ± 0.08^d	42.12 ± 0.13^c	39.46 ± 0.06^b	37.36 ± 0.07^a
Tensile strength (MPa)	20.45 ± 1.13^a	25.31 ± 2.14^a	34.87 ± 3.66^b	32.94 ± 1.29^b	31.89 ± 2.50^b
Elongation at break (%)	40.78 ± 5.29^a	48.75 ± 2.63^a	61.26 ± 1.96^b	67.05 ± 1.98^{bc}	76.10 ± 6.09^c
$L*$	89.69 ± 1.08^e	71.31 ± 1.29^d	86.81 ± 1.57^c	77.21 ± 1.45^b	66.45 ± 2.13^a
$a*$	-2.08 ± 0.14^c	-9.79 ± 1.30^a	-2.06 ± 0.12^c	-7.43 ± 0.93^b	-8.88 ± 1.30^a
$b*$	4.30 ± 0.30^a	-22.38 ± 1.22^d	13.28 ± 1.19^b	14.49 ± 1.76^{bc}	16.03 ± 1.70^c
ΔE	6.73 ± 0.81^a	33.56 ± 0.83^d	15.67 ± 0.55^b	23.55 ± 2.38^c	33.43 ± 1.85^d

Notes: "CS/GA" was the chitosan/gum Arabic film, "A-CS/GA" was the chitosan/gum Arabic film with 3 mg/mL anthocyanin content, "E-CS/GA" was the TO emulsion-chitosan/gum Arabic film, "1A-E-CS/GA" and "3A-E-CS/GA" were the TO emulsion-chitosan/gum Arabic films with 1

mg/mL and 3 mg/mL anthocyanin content.

Table 2 Color variations of the multifunctional packaging films at different pH (3.0-13.0) (Different letters indicate significant difference within one formulation of samples, P < 0.05).

Samples	pH	L^*	a^*	b^*	ΔE	Appearance
CS/GA	3.0	91.14±0.15^{l,m,n}	-1.93±0.04^{i}	4.18±0.05^{a}	5.60±0.11^{a}	
	5.0	91.47±0.07^{l,m,n}	-1.92±0.04^{i}	4.30±0.07^{a}	5.49±0.04^{a}	
	7.0	91.88±0.03^{n}	-1.91±0.05^{i}	4.31±0.14^{a}	5.27±0.11^{a}	
	9.0	91.61±0.10^{mn}	-1.97±0.06^{i}	4.06±0.06^{a}	5.22±0.07^{a}	
	11.0	91.12±0.61^{l,m,n}	-1.95±0.02^{i}	4.00±0.13^{a}	5.50±0.38^{a}	
	13.0	90.45±0.57^{l,m}	-1.97±0.05^{i}	3.84±0.05^{a}	5.82±0.43^{a,b}	
A-CS/GA	3.0	90.98±0.32^{l,m,n}	-0.41±0.07^{m}	5.51±0.19^{b}	6.81±0.34^{b}	
	5.0	88.52±0.42^{k}	-1.22±0.01^{k}	6.44±0.12^{c}	8.99±0.37^{c}	
	7.0	90.33±0.07^{l,m}	-2.69±0.02^{h}	8.27±0.90^{d}	9.57±0.75^{c}	
	9.0	90.22±0.08^{l}	-2.95±0.03^{g,h}	8.34±0.07^{d}	9.70±0.10^{c}	

	11.0	87.2±0.20[j]	-3.70±0.05[f]	10.94±0.18[f]	13.55±0.26[e]
	13.0	91.12±0.05[l,m,n]	-1.83±0.01[i,j]	13.63±0.79[i]	14.25±0.03[e,f]
E-CS/GA	3.0	86.01±0.99[i,j]	-1.91±0.06[i]	12.06±0.58[g,h]	15.00±0.38[f,g]
	5.0	83.75±0.61[g,h]	-1.98±0.05[i]	15.29±0.43[j,k]	18.91±0.70[i]
	7.0	87.13±0.22[j]	-1.97±0.04[i]	13.28±0.23[i]	15.40±0.29[f,g]
	9.0	85.43±0.93[i]	-1.58±0.06[j]	10.95±0.10[f]	14.44±0.54[e,f,g]
	11.0	83.18±0.26[f,g,h]	-1.97±0.07[i]	12.98±0.35[i]	17.43±0.43[h]
	13.0	82.65±0.41[d,e,f,g]	-1.94±0.03[i]	13.67±0.35[i]	18.30±0.41[h,i]
1A-E-CS/GA	3.0	86.26±0.22[i,j]	-0.70±0.04[l]	6.91±0.10[c]	10.97±0.24[d]
	5.0	86.66±0.87[i,j]	-2.14±0.02[i]	8.00±0.67[d]	11.46±0.65[d]
	7.0	78.94±0.63[c]	-3.08±0.14[g]	9.84±0.56[e]	18.68±0.82[i]
	9.0	84.01±0.13[h]	-3.16±0.16[g]	11.07±0.72[f]	15.56±0.60[g]
	11.0	81.45±0.74[d]	-3.23±0.23[g]	12.77±0.29[h,i]	18.56±0.70[h,i]

	13.0	82.00±0.18[d,e,f]	-4.47±0.07[d]	16.06±0.32[k,l]	20.79±0.14[j]	
3A-E-CS/GA	3.0	71.50±1.33[a]	5.50±0.50[o]	10.84±0.58[f]	26.52±1.03[n]	
	5.0	72.10±1.40[a]	2.86±0.29[n]	11.35±0.40[f,g]	25.64±1.45[m,n]	
	7.0	81.86±0.49[d,e]	-4.04±0.09[e]	13.08±0.68[i]	18.59±0.80[h,i]	
	9.0	77.19±0.42[b]	-5.29±0.24[c]	14.78±0.51[j]	23.30±0.38[k]	
	11.0	82.99±0.80[e,f,g,h]	-6.25±0.21[b]	16.26±0.22[l]	20.72±0.50[j]	
	13.0	81.91±0.18[d,e,f]	-6.75±0.09[a]	20.20±0.48[m]	24.60±0.40[l]	

Notes: "CS/GA" was the chitosan/gum Arabic film, "A-CS/GA" was the chitosan/gum Arabic film with 3 mg/mL anthocyanin content, "E-CS/GA" was the TO emulsion-chitosan/gum Arabic film, "1A-E-CS/GA" and "3A-E-CS/GA" were the TO emulsion-chitosan/gum Arabic films with 1 mg/mL and 3 mg/mL anthocyanin content.

FIGURE CAPTIONS

Fig. 1. (A) Schematic diagram of blood orange anthocyanin extraction and multifunctional emulsion-films' fabrication.

Fig. 2. (A) Appearance, (B) structural transformation, (C) UV-visible spectra of the blood orange anthocyanin solutions (3 mg/mL) measured at different pH values (1.0-14.0).

Fig. 3. (A) Light transmittance spectra, (B) water vapor permeability (WVP), and (C) water contact angle of the multifunctional packaging films ("CS/GA" was the chitosan/gum Arabic film, "A-CS/GA" was the chitosan/gum Arabic film with 3 mg/mL anthocyanin content, "E-CS/GA" was the TO emulsion-chitosan/gum Arabic film, "1A-E-CS/GA" and "3A-E-CS/GA" were the TO emulsion-chitosan/gum Arabic films with 1 mg/mL and 3 mg/mL anthocyanin content, different letters indicate significant difference, P < 0.05).

Fig. 4. SEM image of surface and cross-sectional morphologies of the multifunctional packaging films ("CS/GA" was the chitosan/gum Arabic film, "A-CS/GA" was the chitosan/gum Arabic film with 3 mg/mL anthocyanin content, "E-CS/GA" was the TO emulsion-chitosan/gum Arabic film, "3A-E-CS/GA" were the TO emulsion-chitosan/gum Arabic films with 3 mg/mL anthocyanin content, the scale bars were 10 μm, 2 μm, and 1 μm).

Fig. 5. (A) FT-IR spectra, (B) XRD patterns, (C) TGA, and (D) DTG profiles of the multifunctional packaging films ("CS/GA" was the chitosan/gum Arabic film, "A-CS/GA" was the chitosan/gum Arabic film with 3 mg/mL anthocyanin content, "E-

CS/GA" was the TO emulsion-chitosan/gum Arabic film, "3A-E-CS/GA" were the TO emulsion-chitosan/gum Arabic films with 3 mg/mL anthocyanin content.

Fig. 6. (A) Release rate of thyme oil to different food simulants, (B) antioxidant activity, and (C-D) dynamic antibacterial activity of the multifunctional packaging films ("CS/GA" was the chitosan/gum Arabic film, "A-CS/GA" was the chitosan/gum Arabic film with 3 mg/mL anthocyanin content, "E-CS/GA" was the TO emulsion-chitosan/gum Arabic film, "1A-E-CS/GA" and "3A-E-CS/GA" were the TO emulsion-chitosan/gum A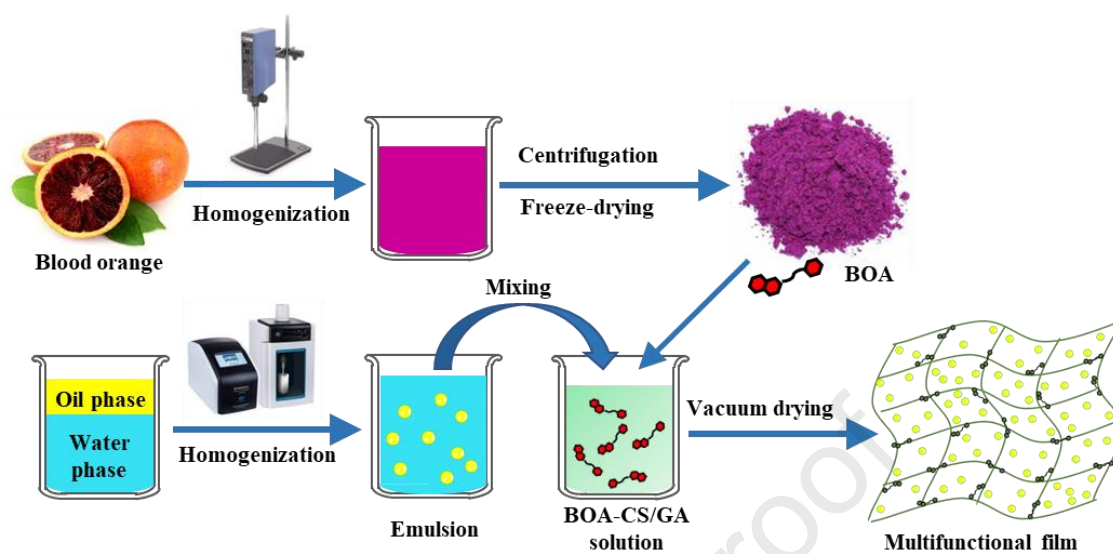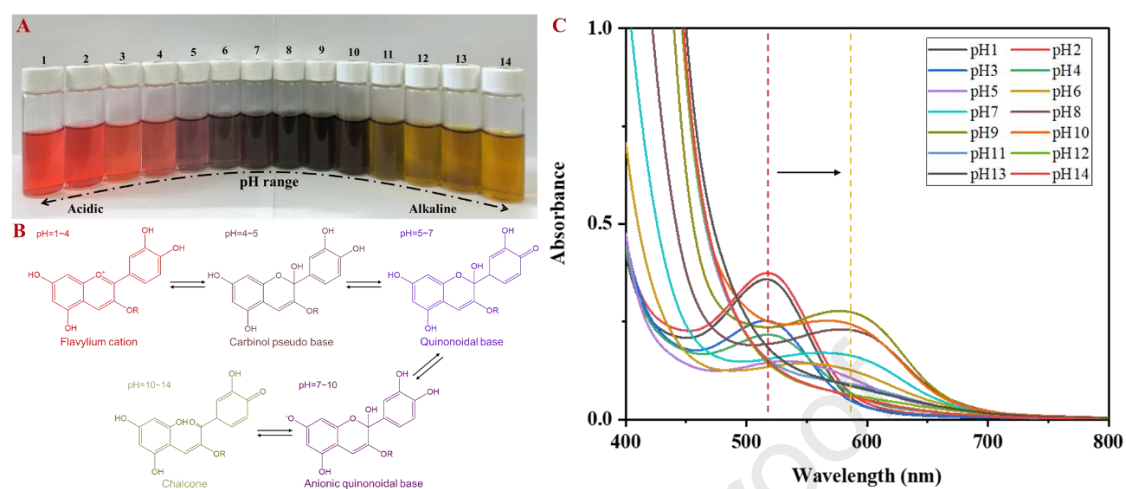rabic films with 1 mg/mL and 3 mg/mL anthocyanin content, different letters indicate significant difference, $P < 0.05$).

Fig. 7. Application of the films to monitoring and maintaining milk freshness: (A-B) Appearance of milk and films (C) pH values and (D) acidity, (E) total bacterial count of milk during storage period, (F-G) color variations (a^*, ΔE) of the multifunctional packaging films during milk storage ("E-CS/GA" was the TO emulsion-chitosan/gum Arabic film, "1A-E-CS/GA" and "3A-E-CS/GA" were the TO emulsion-chitosan/gum Arabic films with 1 mg/mL and 3 mg/mL anthocyanin content).
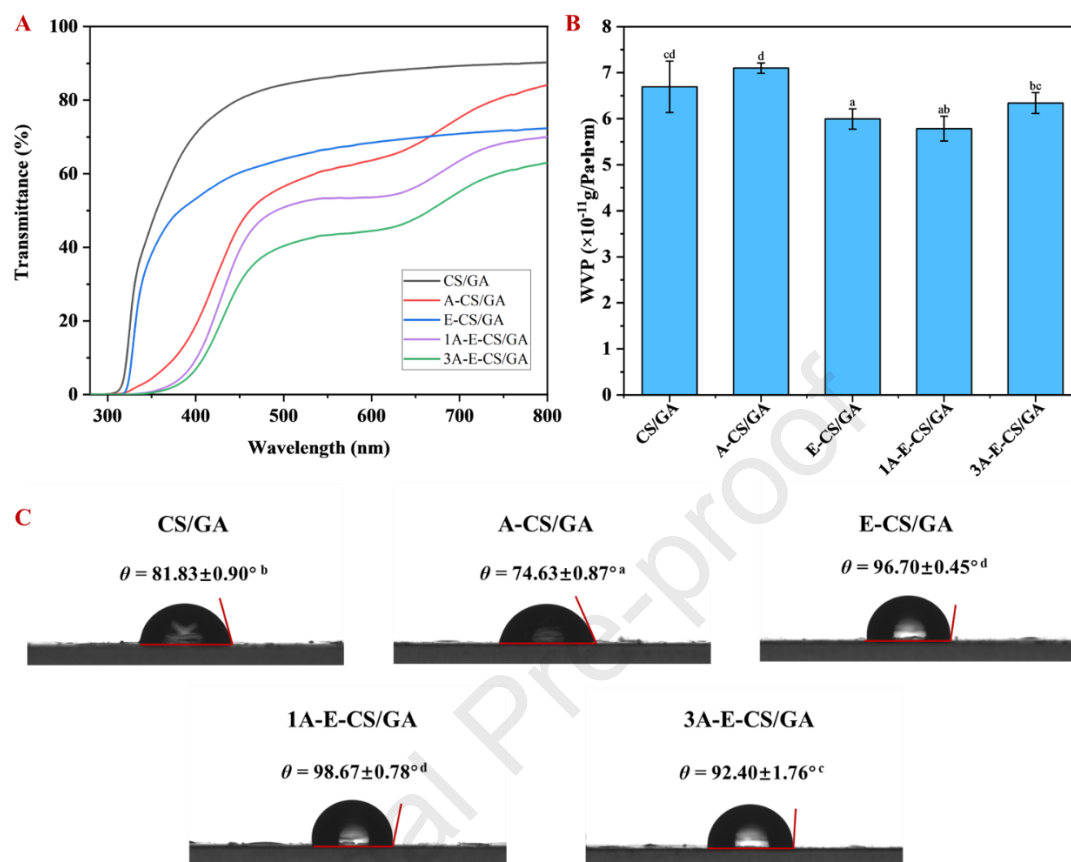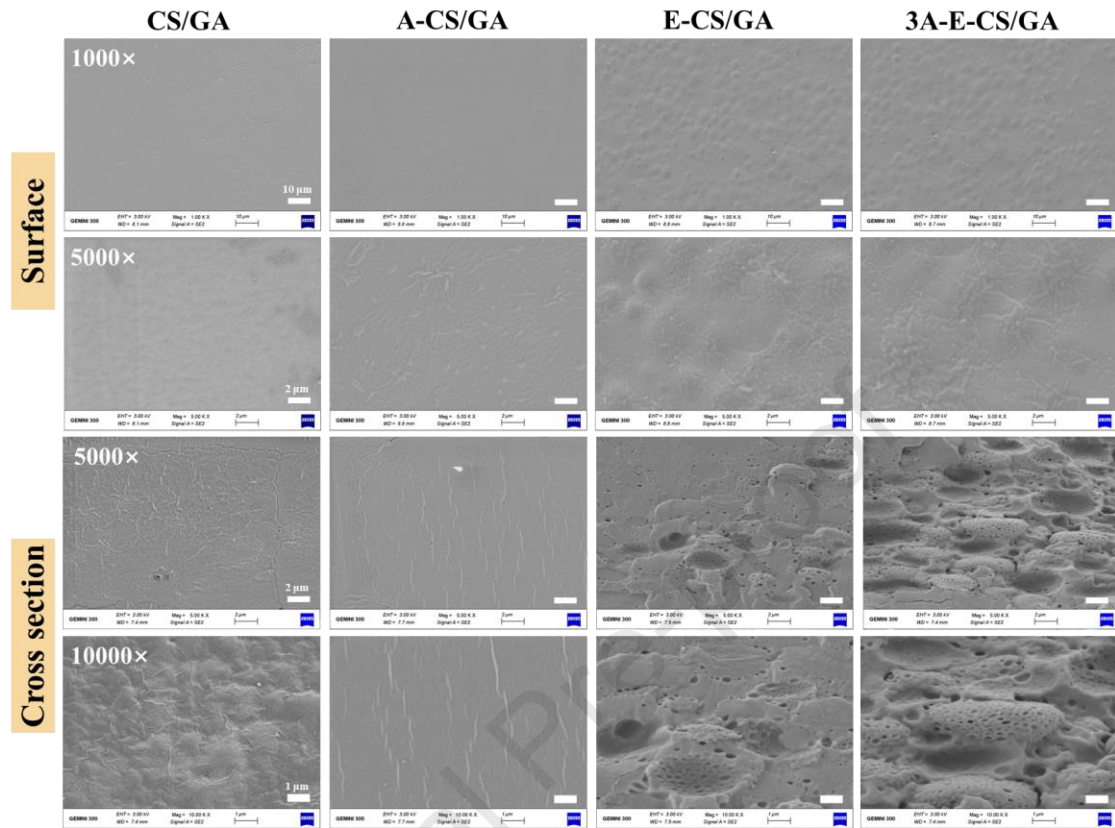
Fig. 1.

Fig. 2.

Fig. 3.

A

B

C

CS/GA	A-CS/GA	E-CS/GA
$\theta = 81.83 \pm 0.90°$ [b]	$\theta = 74.63 \pm 0.87°$ [a]	$\theta = 96.70 \pm 0.45°$ [d]

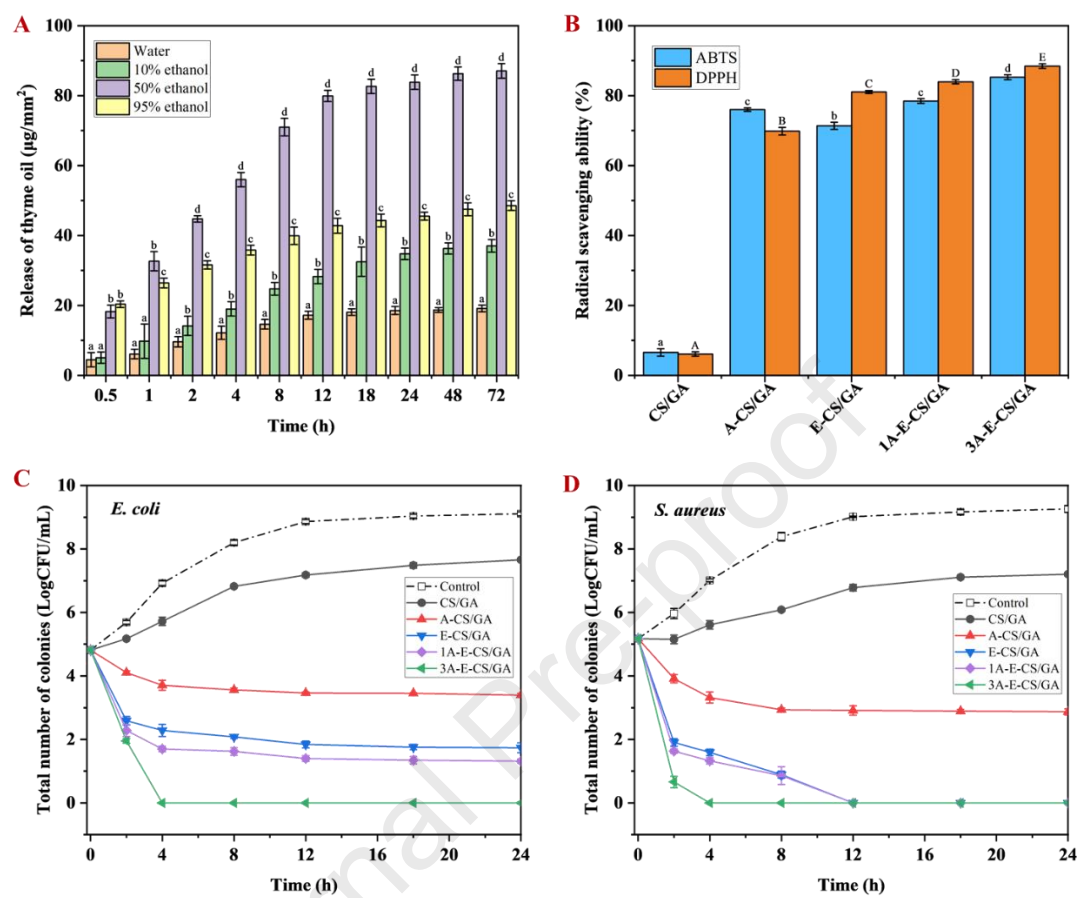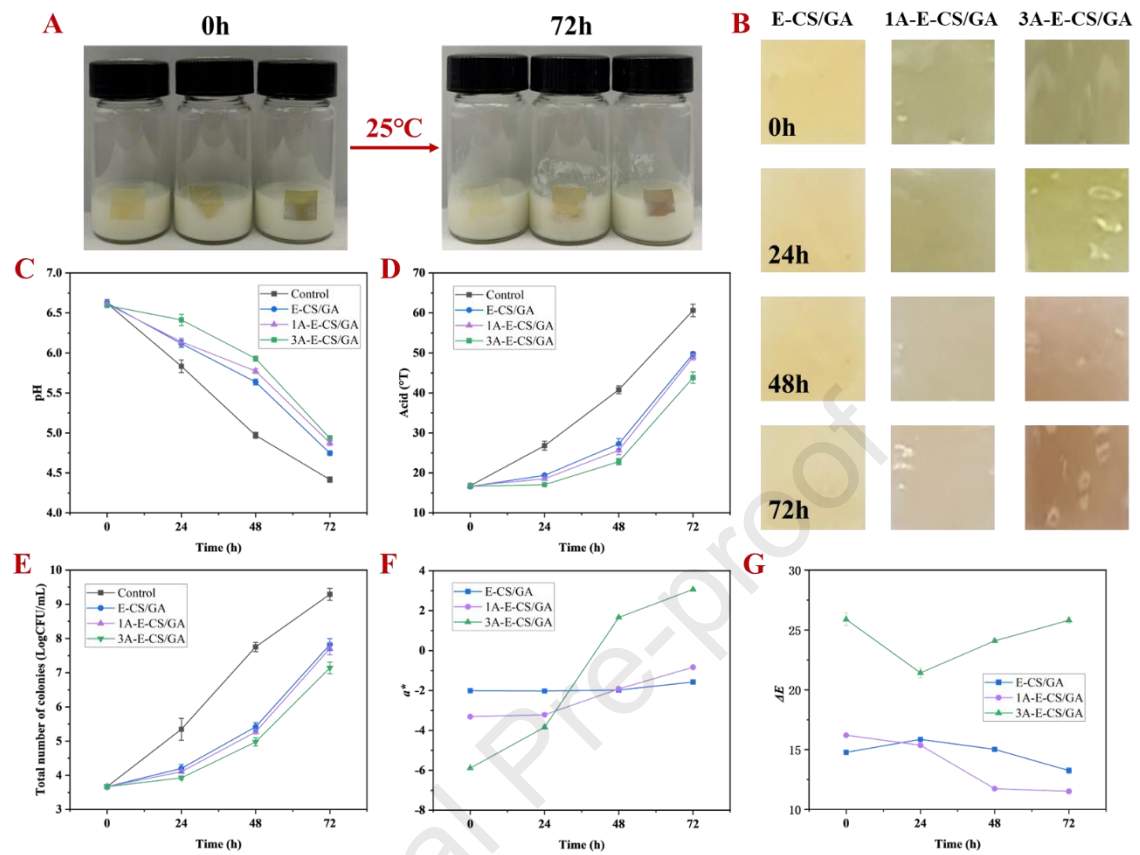| 1A-E-CS/GA	3A-E-CS/GA
$\theta = 98.67 \pm 0.78°$ [d]	$\theta = 92.40 \pm 1.76°$ [c]

Fig. 4.

Fig. 5.
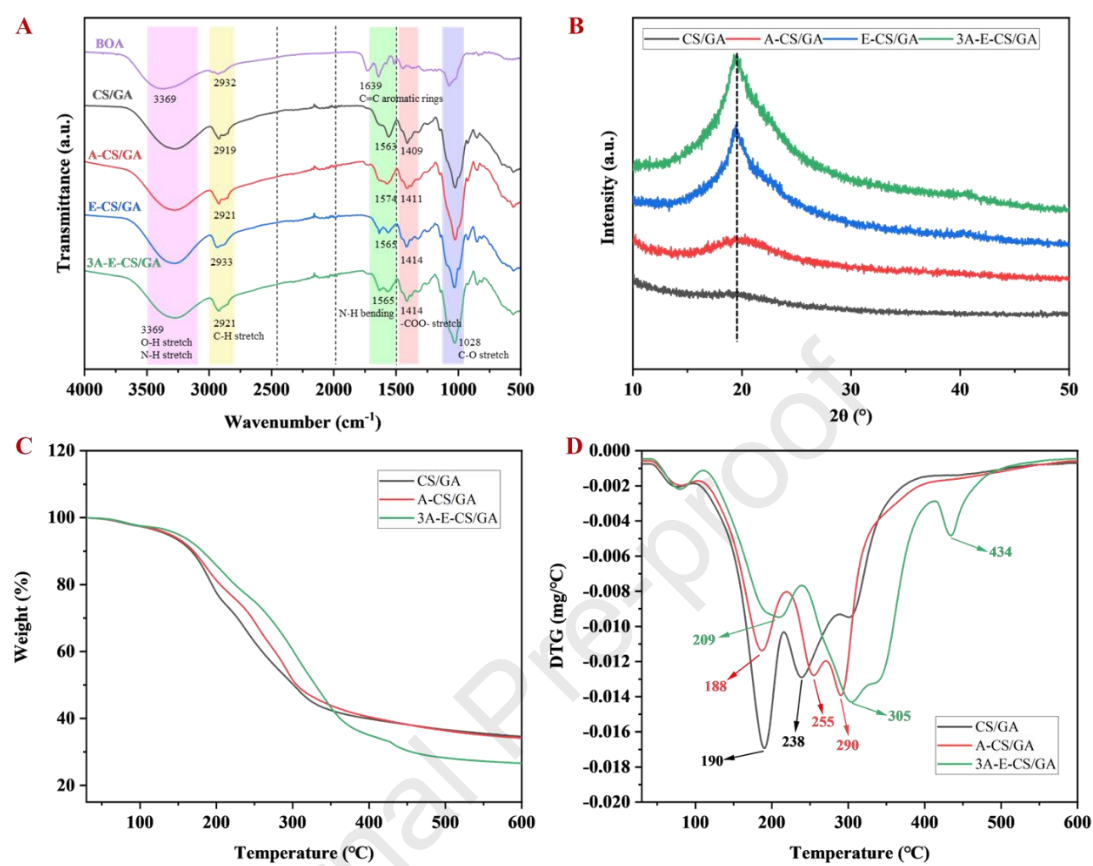
Fig. 6.

Fig. 7.

Highlights

- Blood orange anthocyanins (BOA) were used as pH-sensitive color indicators

- Biopolymer-based films incorporating BOA and TO emulsion were fabricated

- The color of films responded sensitively to acidic/alkaline environment

- The films exhibited excellent antioxidant and antibacterial properties

- The films can be used to prolong and visually monitor the food freshness

Declaration of interests

☒ The authors declare that they have no known competing financial interests or personal relationships that could have appeared to influence the work reported in this paper.

☐The authors declare the following financial interests/personal relationships which may be considered as potential competing interests: